Pinning characteristics in chemically modified (Nd, Eu, Gd)–Ba–Cu–O superconductors

M. Muralidhar,[a] N. Sakai, M. Nishiyama, M. Jirsa,[b] T. Machi, and M. Murakami
Superconductivity Research Laboratory (SRL), International Superconductivity Technology Center, Division 3, 1-16-25, Shibaura, Minato-ku, Tokyo 105-0023, Japan

(Received 29 July 2002; accepted 6 December 2002)

In melt-processed $(Nd_{0.33}Eu_{0.38}Gd_{0.28})Ba_2Cu_3O_y$ (NEG-123) materials we found a new type of nanometer-scale pinning defects. Structural analysis was made with a dynamic force microscope and a scanning tunneling microscope (STM) that both showed the formation of a nanometer-scale lamellar structure. The high magnification STM showed that the nanolamellas are in fact rows (or planes) of aligned NEG-rich clusters 3–4 nm in size. This new pinning medium led to an increase of B_{irr} at 77 K for the $H_{\parallel} c$ axis up to 12 T (measured by a superconducting quantum interference device) or 15 T (measured by a vibrating sample magnetometer). A secondary peak as high as 70 kA/cm^2 was observed at 4.5 T and decreased to 49 and 22 kA/cm^2 at 7 and 10 T, respectively. [DOI: 10.1063/1.1542927]

As already shown in several reports,[1–5] $(Nd_{0.33}Eu_{0.38}Gd_{0.28})Ba_2Cu_3O_y$ (NEG-123) bulk superconductors exhibit superior pinning characteristics, uniform microstructure and good reproducibility. For applications in temperatures at and above 77 K, however, a further pinning enhancement, especially in high magnetic fields, is needed. Recently, it was found that a distinct range of the rare earth chemical ratio in the $(Nd,Eu,Gd)Ba_2Cu_3O_y$ system strongly affected the pinning properties at high fields.[6] A proper choice of the Nd: Eu: Gd ratio enabled manipulation of the secondary peak position in the range of 1–4 T at 77 K, a corresponding change of the irreversibility field, and control of the secondary peak height.[7] The relative content of Eu in the NEG matrix was crucial for control of the irreversibility field and the secondary peak position. In samples rich in Gd the secondary peak of magnetization was high (reaching nearly 10^5 A/cm^2), relatively narrow, and appeared at relatively low fields.[6] According to Kramer,[8] narrowing of the secondary peak and shifting toward lower fields are overall consequences of pinning enhancement in a system where vortex clusters shear between islands of strongly pinned vortices. Although large deviations from Kramer's rule have been observed, we can conclude that the Gd enrichment caused an increase of point-like disorder.

In this work we focused on a narrow range of the NEG compositions, enriched in Eu, which exhibit high irreversibility fields. An attempt was made to correlate magnetic properties with microstructure characteristics.

High-purity commercial powders of Nd_2O_3, Eu_2O_3, Gd_2O_3, $BaCO_3$ and CuO were mixed in a nominal composition of $(Nd_{0.33}Eu_{0.38}Gd_{0.28})Ba_2Cu_3O_y$. The starting powder mixtures were thoroughly ground, calcined at 880 °C for 24 h with intermediate grinding, pressed into pellets and sintered at 900 °C for 15 h under oxygen partial pressure (pO_2) of 0.1% O_2. The whole procedure was repeated three times. Then commercial Nd-422, Eu-211, and Gd-211 powders were mixed in a ratio of 1:1:1 and added to the sintered NEG-123 powders in concentrations of 3 and 40 mol % of NEG-211, together with 0.5 mol % of Pt for 211 phase particle refinement and 10 wt % of Ag_2O to improve mechanical properties. Finally, pellets of 20 mm diameter and 15 mm thickness were prepared by cold isostatic pressing at 200 MPa. All samples were fabricated by the oxygen controlled melt growth (OCMG) process at pO_2 of 0.1% and gas flow rate of 300 ml/min. Details of the heat treatment schedule can be found elsewhere.[1]

For magnetic measurements small specimens with dimensions of $a\times b\times c = 1.5\times 1.5\times 0.5$ mm^3 were cut from the pellets and annealed in flowing oxygen in the temperature range of 300–600 °C.[1] The microstructure of these samples was studied with a dynamic force microscope (DFM) and scanning tunneling microscope (STM). The chemical composition of the matrix was analyzed by energy dispersive x-ray (EDX) spectroscopy. Magnetization hysteresis loops ($M-H$ loops) in fields from -2 to $+7$ T were measured at 77 K using a commercial superconducting quantum interference device (SQUID) magnetometer (Quantum Design, model MPMS7). J_c values were estimated based on the extended Bean critical state model for a rectangular sample.[9]

Figure 1 shows the magnetization measurements of $(Nd_{0.33}Eu_{0.38}Gd_{0.28})Ba_2Cu_3O_y$ samples with 3, 5, 10, 20, and 40 mol % NEG-211 measured at 77 K with the field applied parallel to the c axis. A clear secondary peak effect was observed in most of the samples. $M(H_a)$ curves for the sample with 3 and 40 mol % NEG-211 showed a plateau instead of the peak in intermediate fields. All the samples with the intermediate contents of 211 phase exhibited an irreversibility field, B_{irr}, that exceeded 7 T. The consistent results of the whole set of compositions convinced us that an increase in the irreversibility field originated from the particular chemical ratio in the NEG-123 matrix in combination with an appropriate amount of secondary phase. In the present system, the concentration of 5 mol % NEG-211 proved to be optimal, resulting in the highest irreversible

[a]Electronic mail: miryala1@istec.or.jp
[b]Also at Institute of Physics, ASCR, CZ-182 21 Praha 8, Czech Republic.

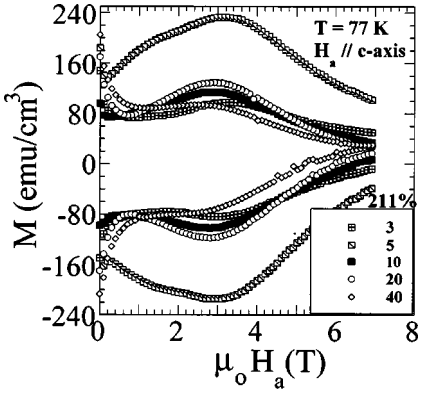

FIG. 1. Field dependence of the magnetization measured with a SQUID magnetometer at $T=77$ K, with $H_a \| c$ to the axis, for $(Nd_{0.33}Eu_{0.38}Gd_{0.28})Ba_2Cu_3O_y$ superconductors with 3, 5, 10 20 and 40 mol % NEG-211. Note the high irreversibility field and a slight additional maximum between the first and secondary peaks in the sample with 5 mol % NEG-211.

moment at 7 T (the maximum field of our SQUID magnetometer). In order to determine the actual B_{irr} value, we made magnetization measurements by means of a vibrating sample magnetometer (VSM) with maximum field of 14 T. The magnetization hysteresis loop for the latter sample measured with a field sweep rate of 0.6 T/min at 77 K is shown in Fig. 2 (top). Note that the effective field sweep rates and the associated relaxation states of the sample significantly differ when measured with the SQUID and VSM, which affects the resulting B_{irr} values and makes them incomparable.[10] However, the scaling property can help us to bring the values into accord. It is well known[10] that the secondary peak position, B_p, scales approximately with B_{irr}. By comparing Figs. 1 and 2 (top) one can determine the factor of the change in B_p due to the field sweep effect to about $4.2T/3.3T=1.27$. This

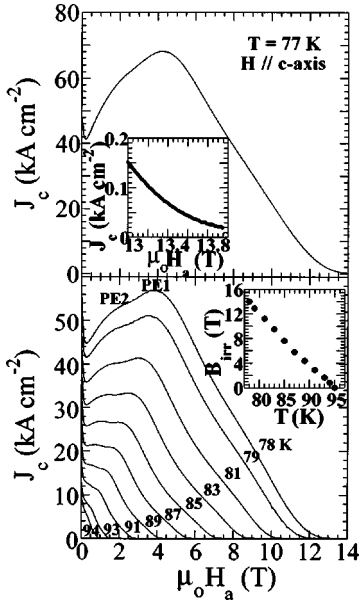

FIG. 2. Field dependence of the critical current density (J_c) for the $(Nd_{0.33}Eu_{0.38}Gd_{0.28})Ba_2Cu_3O_y$ sample with 5 mol % NEG-211 measured with a VSM at 77 K ($H \| c$) at field sweep rate of 0.6 T/min (top). The top inset shows that the irreversible field exceeds 14 T. Current density vs $H_a(T)$ measured at various temperatures for the same sample (bottom). The bottom inset shows the extrapolated value of B_{irr} to be around 15 T at 77 K, $H \| c$ axis.

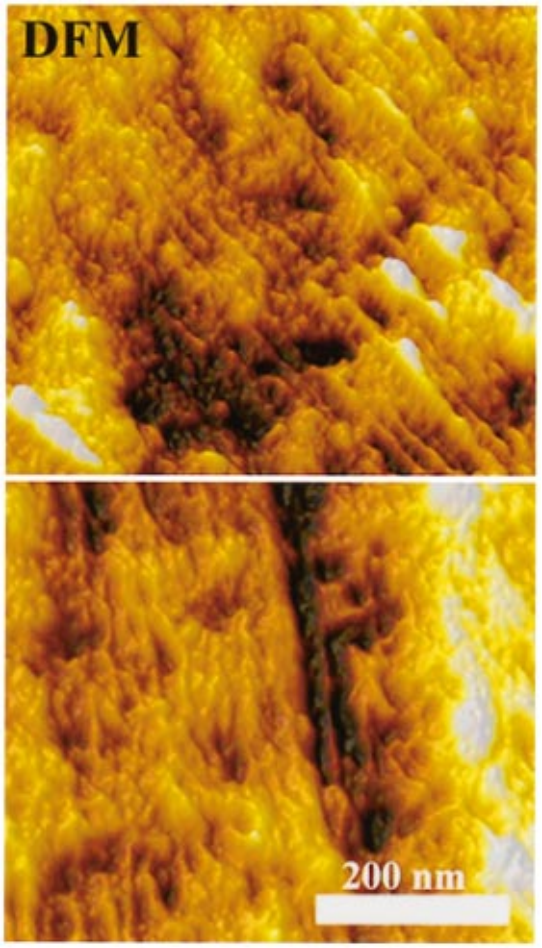

FIG. 3. (Color) Dynamic force microscope images of the $(Nd_{0.33}Eu_{0.38}Gd_{0.28})Ba_2Cu_3O_y$ sample with 5 mol % NEG-211. Note the nanolamellar (upper micrograph) and modulation structure (lower micrograph). Both features were observed in several samples.

factor should control also the corresponding change of B_{irr}. As shown in inset of Fig. 2 (bottom), extrapolation of the $B_{\mathrm{irr}}(T)$ data measured at temperatures $78\ \mathrm{K} \leqslant T \leqslant 95$ K gives the VSM value of $B_{\mathrm{irr}}(77\ \mathrm{K}) \approx 15$ T. An adequate value of B_{irr} for comparison with SQUID data should be about $15T/1.27$, i.e., about 12 T. Even this value is significantly higher than in other compounds at 77 K and makes the new material an excellent candidate for high field applications.

The critical current density, J_c, in the (a,b) plane obtained from the extended Bean model is presented in Fig. 2 (bottom). Critical current densities associated with the secondary peak reached 70, 49 and 22 kA/cm^2 at 4.5, 7 and 10 T, respectively (VSM data with a field sweep rate of 0.6 T/min). The $J_c(B)$ curves in Fig. 2 show two secondary peaks, PE1 and PE2, a typical result of a combination of a point-like structure with twin planes. This can also be interpreted as a regular broad secondary peak flattened by twin structure activity.[11] The temperature scan shows that the maximum of PE2 (or the low-field edge of secondary peak flattening) becomes with an increase in temperature more pronounced but only insignificantly shifts toward lower fields. On the other hand, peak PE1 (or the high-field edge of secondary peak flattening) rapidly diminishes with an increase in temperature and shifts toward low fields as a regular secondary peak. As PE1 comes close to PE2, both peaks

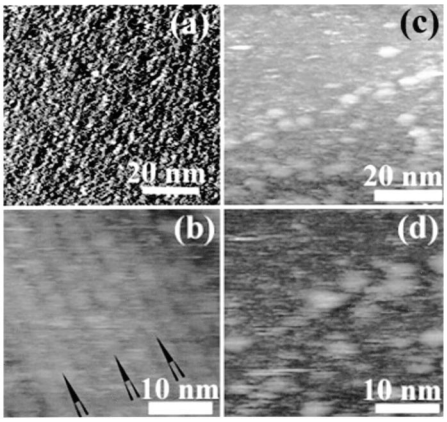

FIG. 4. STM image of the cleaved surface of $(Nd_{0.33}Eu_{0.38}Gd_{0.28})Ba_2Cu_3O_y$ with 5 (a), (b) and 40 mol % NEG-211 (c), (d). The tunneling conditions were $V_s = 10$ V and $I_t = 0.3$ nA. Note that the modulation (a) and nanolamellar structures (b) are similar to the DFM micrographs. The black arrows in (b) show some nanolamellaes, with the average period around 3.5 nm. Both nanostructures were absent in the sample with 40 mol % NEG-211 (c), (d).

merge and the resulting singular peak shifts toward low fields and finally disappears. Similar effects have also been observed in Nd-123 single crystals.[12] Angular experiments also proved that deformation of the $M-H$ curves was really due to a planar pinning structure aligned with the c axis.

In order to clarify reasons for the improved magnetic properties, we observed the microstructure of the $(Nd_{0.33}Eu_{0.38}Gd_{0.28})Ba_2Cu_3O_y$ sample with 5 mol % NEG-211. We prepared the specimens for observation by polishing samples from the same batch used for magnetic measurements. Figure 3 shows the DFM image of the sample with 5 mol % NEG-211 viewed from the [001] direction. Significant in this image is the nanoscale lamellar (top) and modulation structure (bottom). We observed both features in several samples. A similar type of microstructure was also observed in the sample with 3 mol % of NEG-211. This sample showed a high irreversibility field at 77 K (see Fig. 1). On the other hand, no such nanostructure was observed in the sample with 40 mol % NEG-211 and the magnetic performance of this sample at 77 K was nearly equal to that of $(Nd_{0.33}Eu_{0.33}Gd_{0.33})Ba_2Cu_3O_y$.[1] Both the magnetization data and DFM results suggest that the nanoscale microstructure is responsible for the high irreversibility at 77 K.

In order to learn more about the new type of nanoscale microstructure, we performed ultrahigh vacuum (UHV) STM measurements at room temperature on NEG-123 samples with 5 and 40 mol % NEG-211. The samples exhibited very high and low irreversibility fields, respectively. Figures 4(a) and 4(b) show STM images of the NEG-123 sample (Nd:Eu:Gd = 33:38:28) with 5 mol % of NEG-211. Figures 4(a) and 4(b) show, respectively, the modulation and the nanolamellar structure. The modulation period is about 4 nm, which is comparable to the coherence length [in YBCO (77 K) = 4.5 nm]. Such a structure can principally change the vortex dynamics and pinning efficiency at high fields. A careful check of Fig. 4(b) revealed a nanolamellar structure along the modulation direction. No structure of this kind was identified in the sample with 40 mol % NEG-211 [see Figs. 4(c) and 4(d)].

The local chemical composition of the matrix mapped by TEM/EDX revealed fluctuating (Nd + Eu + Gd)/Ba substitution in the 123 matrix. It seems that fluctuations contribute to the point-like pinning disorder.[13,14] On the other hand, the tunneling current spectra show similar conductivity on nanoscale lamellae and the regular matrix. This is probably due to the fact that the RE-rich $Re_{1+x}Ba_{2-x}Cu_3O_y$ (RE-123ss) clusters have a composition not much different from that of the 123 matrix. In the case of Nd-123 single crystals, an island structure with a Ba^{2+} site in Nd-123 partially occupied by Nd^{3+} ions was identified.[14] The typical period was in this case much bigger (tens of nanometers) than what we observed here. Note that thin plate-like domains with 8 nm period were also observed in Pb-doped $Bi_2Sr_2CaCu_2O_y$ single crystals and their appearance was attributed to spatial variation in the Pb content.[15] Also in this case, pinning at high fields and temperatures was significantly improved.

In conclusion, bulk $(Nd_{0.33}Eu_{0.38}Gd_{0.28})Ba_2Cu_3O_y$ samples doped with 3–40 mol % of NEG-211 were prepared by the OCMG process. In a narrow range of Nd:Eu:Gd ratio pinning at high fields was significantly enhanced: the irreversible field at 77 K reached 12 T (measured by SQUID) and 15 T (measured by VSM), and J_c maintained sufficient values for industrial applications up to 10 T. The STM and DFM analyses revealed a nanoscale laminar structure with a period comparable to the coherence length that is most probably responsible for the pinning enhancement.

This work was supported by the New Energy and Industrial Technology Development Organization (NEDO) as Collaborative Research and Development of Fundamental Technologies for Superconductivity Applications. One of the authors (M.J.) acknowledges support from Grant No. A1010919/99 of Grant Agency of Academy of Science of the Czech Republic.

[1] M. Muralidhar, M. R. Koblischka, T. Saitoh, and M. Murakami, Supercond. Sci. Technol. **11**, 1349 (1998).
[2] M. Muralidhar, M. Murakami, K. Segawa, K. Kamada, and T. Saitho, U.S. Patent No. 6,063,753 (2000).
[3] A. K. Pradhan, M. Muralidhar, M. R. Koblischka, M. Murakami, K. Nakao, and N. Koshizuka, Appl. Phys. Lett. **75**, 253 (1999).
[4] M. Muralidhar, M. R. Koblischka, P. Diko, and M. Murakami, Appl. Phys. Lett. **76**, 91 (2000).
[5] M. R. Koblischka, M. Muralidhar, and M. Murakami, Appl. Phys. Lett. **73**, 2351 (1998).
[6] M. Muralidhar and M. Murakami, Phys. Rev. B **62**, 13911 (2000).
[7] M. Muralidhar, M. Jirsa, N. Sakai, and M. Murakami, Appl. Phys. Lett. **79**, 3107 (2001).
[8] E. J. Kramer, J. Appl. Phys. **44**, 1360 (1973).
[9] D. X. Chen and R. B. Goldfarb, J. Appl. Phys. **66**, 2489 (1989).
[10] M. Jirsa, M. Muralidhar, M. Murakami, K. Noto, T. Nishizaki, and N. Kobayashi, Supercond. Sci. Technol. **14**, 50 (2001).
[11] M. Jirsa, M. R. Koblischka, T. Higuchi, and M. Murakami, Phys. Rev. B **58**, R14771 (1998).
[12] Th. Wolf, A.-C. Bornarel, H. Kupfer, R. Meier-Hirmer, and B. Obst, Phys. Rev. B **56**, 6308 (1997).
[13] T. Egi, J. G. Wen, K. Kurada, N. Koshizuka, and S. Tanaka, Appl. Phys. Lett. **67**, 2406 (1995).
[14] W. Ting, T. Egi, K. Kurada, K. Koshizuka, and S. Tanaka, Appl. Phys. Lett. **70**, 770 (1997).
[15] I. Chong, Z. Hiroi, M. Izumi, J. Shimoyama, Y. Nakayama, K. Kishio, T. Terashima, Y. Bando, and M. Takano, Science **276**, 770 (1997).